Premixed Flame Propagation Characteristics in a Supersonic Airstream

A.M. Agnone*
New York University, Westbury, N.Y.
and
G.Y. Anderson†
NASA Langley Research Center, Hampton, Va.

Nomenclature

A_f = flame cross-sectional area $= \pi r_f^2$
L = length
M = Mach number
$\dot{m}$ = mass flow rate
p = pressure
r_f = radial distance to flame height
$r_{1/2}$ = half radius
T_0 = maxture stagnation temperature
u = velocity
v_N = flame propagation speed
w = width
y_{H_2O} = water mass fraction
ϵ = flame entrainment rate
$\bar{\theta}_f$ = average flame angle
μ = viscosity
ρ = density
φ = equivalance ratio

Subscripts

0 = centerline
e = edge
b = burned
u = unburned

Introduction

TO implement the design of premixed combustion chambers, it is necessary to be able to predict the flame propagation characteristics. At flow conditions typical of scramjet combustors, only a few premixed combustion experiments are available to assess the reliability of theoretical predictions. Measured values of flame angles are presented here. A comparison of these data with a theoretical analysis is conducted to correlate the flame spread, velocity, and burning rate dependence on the unburned flow properties and turbulence levels.

Experimental Apparatus

Premixed hydrogen and air flame propagation tests were conducted at NASA Langley Research Center as a follow-on to results presented in Ref. 1. These tests used a set of contoured plug nozzles (axisymmetric) designed to produce uniform exit flow with the flow at the pilot exit parallel to the centerline (Fig. 1). The details of the experimental apparata are presented in Refs. 1 and 2. Tests were conducted with Mach number 1.3 and 2.5 nozzles for nominal mixture stagnation temperatures of 270 and 470 K over a range of equivalence ratio. For all tests, the plenum pressure is adjusted to make the exit pressure equal to the ambient pressure. At these conditions the flame was predominantly turbulent.

Data Presentation

Figure 2 presents the measured average flame angles‡ vs equivalence ratio, φ, for $M=1.3$, and for mixture stagnation temperature, $T_{0_{mix}} = 270$ K and 470 K. The scatter at $\varphi < 1$ could not be resolved. The data points with an arrow indicate an unstable flow was obtained.

The flame angle data for $M=2.5$, is also shown in Fig. 2. Unsteady rough burning was encountered at the $T_0 = 270$ K condition. The combustion was much more stable at $T_0 = 470$ K than at $T_0 = 270$ K.

The present data and that presented in Ref. 1 are correlated with the square root of the stagnation temperatures of the unburned mixture stream in Figs. 3a and 3b for the $M=1.3$ and 2.5 conditions respectively. The data obtained in Ref. 1 is shown in Fig. 3c. These indicate that the flame angle is inversely proportional to the square root of the mixture stagnation temperature. Or, for the same Mach number, it is inversely proportional to the mixture speed. Also shown in Figs. 3a, b, and c are several theoretical curves. The solid curve was obtained by assuming the flame angle to be proportional to the amount of heat released (i.e., amount of water produced) assuming complete combustion across the flame. The proportionality constant was adjusted with the experimental data at fuel-rich conditions ($\varphi \sim 1.5$). The water mass fraction, Y_{H_2O}, was obtained from equilibrium chemistry tables. The experimental flame angles are consistently greater than these values. The discrepancy is due to additional heat release produced by the fuel rich combustion products of the air-hydrogen-oxygen pilot.

The dashed curves shown in the figures were calculated theoretically with a computer program (Refs. 3 and 4) using finite rate chemistry, constant pressure, and several levels of eddy viscosity greater than a nominal level $\mu_0 \sim 1 \times 10^{-4}$ slugs/sec/ft $= 0.0285\ r_{1/2}\rho_0 u_0$. Again the experimental flame angle data is consistently greater than the theoretical level. The slope of the flame angle vs equivalence ratio curve is steeper in the case of the finite rate than the equilibrium case. Also, with finite rate chemistry, the curve does not level off at fuel-rich conditions. A comparison of the curves for the three different Mach number conditions shows an increasing level of turbulent eddy viscosity with increasing Mach number.

The calculated values of the flame speed ($v_N = \rho_b / \rho_u v_b \sin\theta_f$) are shown in Fig. 4 as a function of the equivalence ratio for the $T_0 = 470$ K condition and for the three different Mach numbers. The dashed curves are the variation of the flame speed nondimensionalized with respect to the unburned mixture stream velocity. The data of Ref. 1 does not appear consistent with the present data. This may be due to the fact that in Ref. 1, a different apparatus was used which caused an initial shock at the ignitor lip, that produced a local pressure rise which subsequently decayed to the ambient pressure. Therefore the combustion was not isobaric.

The flame burning rate (i.e., mixture entrainment rate per unit of cross-section flame area, $\epsilon = d\dot{m}/dA_f$) is shown in Fig. 5, nondimensionalized with respect to the mixture stream mass flux per unit area $\rho_e u_e$, as a function of the equivalence ratio for the 470 K mixture stagnation temperature and two different Mach numbers. This shows that the nondimensionalized burning rate is greater at the lower speed and is a minimum at stoichiometric conditions.

Conclusions

The data presented here shows that the premixed flame angle is proportional to the amount of heat released. Also the flame angle is easily correlated with the fuel mixture ratio

Received Dec. 10, 1976; revision received Feb. 7, 1977.
Index categories: Reactive Flows; Combustion in Gases.

*Senior Research Scientist. Member AIAA.

†Head of Components Section of Hypersonic Propulsion Branch. Member AIAA.

‡The average flame angle was obtained from schlieren photo negatives of the flowfield by measuring the average flame spread at a given distance, L, (Fig. 1) from the ignitor. Time average schlieren exposures were used (Ref. 1). The results with this technique agree well with other methods of obtaining the flame angle from schlieren negatives. The time average schlieren technique gives a good representation of the brightest region of the flame zone.

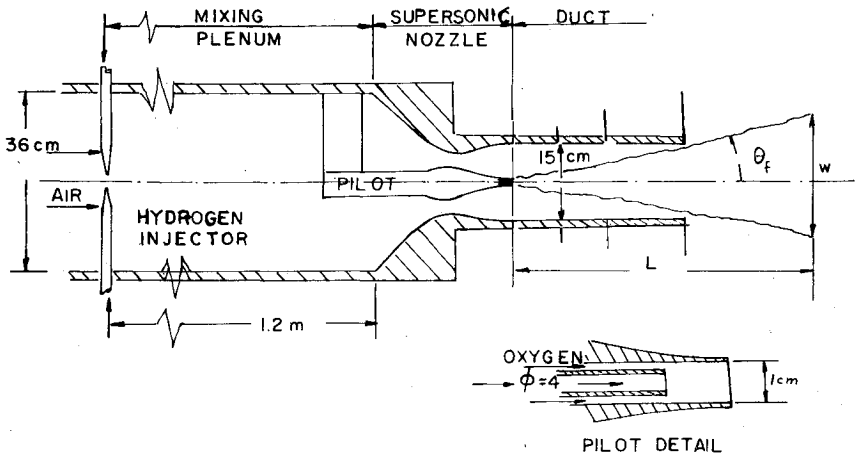

Fig. 1 Schematic of experimental apparatus.

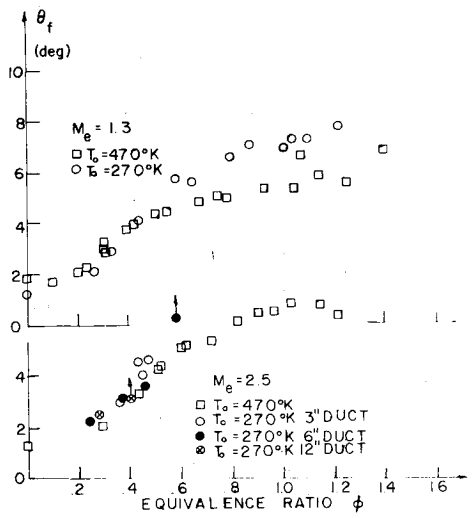

Fig. 2 Measured values of mean flame angle.

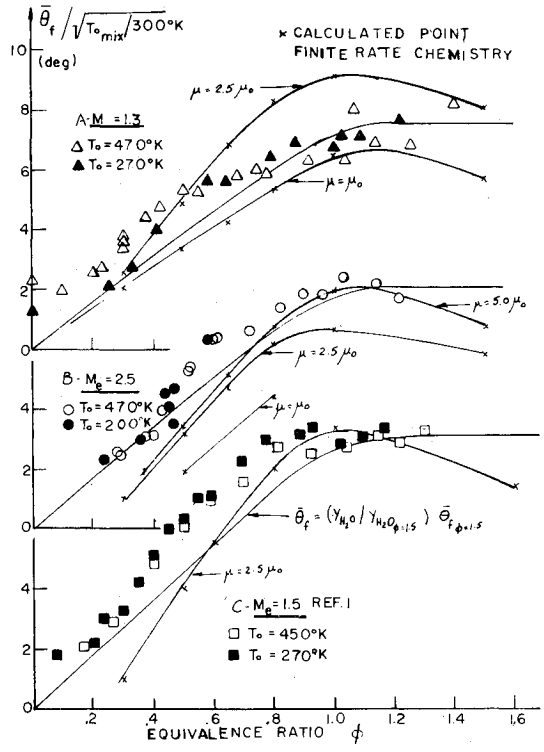

Fig. 3 Comparison of measured flame angles with analysis.

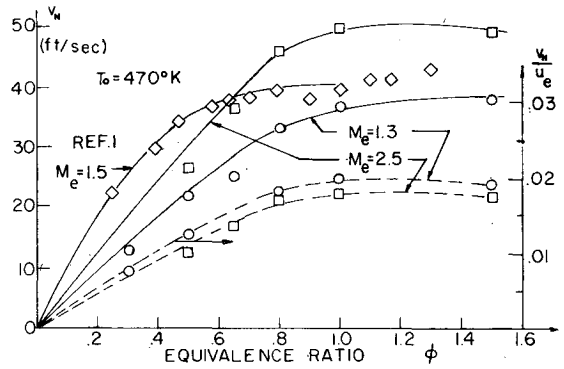

Fig. 4 Flame propagation velocity.

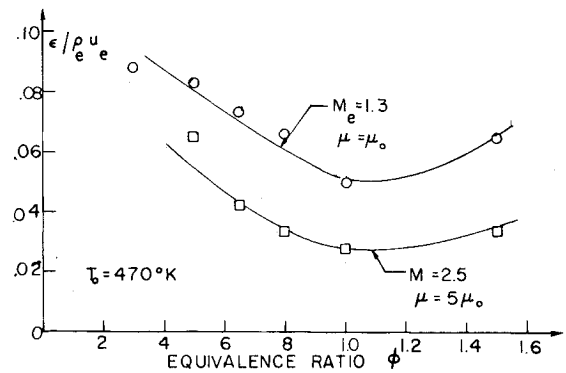

Fig. 5 Nondimensional burning rate.

through the heat release or water formation rates. The effects of finite rate combustion on the flame angle predominate at off-stoichiometric conditions. The pilot affects the flame angle if a significant amount of unburnt fuel is present in the pilot hot gases. The level of viscosity is several times the nominal level, being greater at the higher unburnt mixture Mach number.

Acknowledgment

The work reported herein was supported by the National Aeronautical and Space Administration under Grant No 1 NGR-33-016-131.

References

[1]Anderson, G.Y. and Vick, A.R., "An Experimental Study of Flame Propagation in Supersonic Premixed Flows of Hydrogen and Air," NASA TN D-4631, June 1968.

[2]Eggers, J.M., "Turbulent Mixing of Co-Axial Compressible H_2-Air Jets," NASA TN D-6487, Sept. 1971.

[3]Edelman, R. and Fortune, O., "A Preliminary Analysis of Mixing and Combustion in Ducted Flows with Application to Ejector Ramjet Technology," General Applied Science Laboratories, Westbury, N.Y., GASL Technical Report No. 658, May 1967.

[4]Siegelman, D. and Fortune, O., "Computer Programs for the Mixing and Combustion of Hydrogen in Air Streams," General Applied Science Laboratories, Westbury, N.Y., GASL Technical Report No. 618, July 1966.

Momentum Transfer to a Surface with a Pulsed Laser

Peter K. Wu* and Peter E. Nebolsine†
Physical Sciences Inc., Woburn, Mass.

Introduction

THE phenomenology of laser material interaction has been of interest for many years and the momentum transfer to a surface by a laser beam has been reported by many investigators.[1-4] This Note will examine the transient momentum transfer in vacuum in the "transparent" limit, where the laser intensity is below the threshold for plasma formation. In vacuum, particulates may come directly from the surface as a result of laser energy deposition and cause vapor breakdown, a complex phenomenon. Schlier, et al.[5] has reported thresholds of order 10^6 W/cm^2 for large 20μ particles for laser pulse width $\sim 10^{-5}$ sec. Here we will consider intensities below this level. Previous studies were concerned primarily with high intensity laser beams.[1-4] In this regime, when solids are irradiated either in vacuum or atmospheric conditions, plasma is formed above the surface and may degrade the efficiency of momentum transfer to the solid.

A. Transient Heat Conduction

A one-dimensional transient heat conduction problem has been formulated for carbon phenolic, and the governing equation can be written as

$$\rho C_p \frac{\partial T}{\partial t} = K\frac{\partial^2 T}{\partial x^2} + (C_p)_g \dot{m}_g \frac{\partial T}{\partial x} + Q_g \dot{W}_g \qquad (1)$$

where ρ is the density of solid; C_p is the specific heat of solid; T is the temperature; t is the time, $(C_p)_g$ is the specific heat of pyrolyzed (resin) gas; $\dot{m}_g$ is the mass flux of pyrolyzed gas; Q_g is the enthalpy of pyrolysis per unit mass of gas generated; $\dot{W}_g$ is the rate of gas generation per unit volume; and x is the axial coordinate. The last two terms represent the energy transfer due to internal gasification (pyrolysis). Equation (1) has been solved by an explicit forward-marching technique in finite difference form with the initial condition $T(x,t=0)=T_0(x)$ and the boundary conditions for $t>0$

$$-K\frac{\partial T}{\partial t} = I_0 - \dot{m}\Delta H - \epsilon\sigma T^4 - \frac{\rho C_p \Delta T}{\Delta t}, \quad x=0$$

$$\frac{\partial T}{\partial x} = 0 \qquad x=L$$

where $\dot{m}$ is the vaporization rate at the surface; ΔH is the heat of vaporization $(=2.6\times 10^4 Kj/Kg)$[6]; ϵ is the emissivity; σ is the Stefan-Boltzmann constant; and I_0 is the laser flux. The pyrolysis reaction rate can be expressed as[6]

$$W_g = A\rho_r^2 \exp\{-(E/RT)\}$$

where A is a constant; ρ_r is the resin density; E is the activation energy of pyrolysis; and R is the gas constant. The resin density is given by

$$\rho_r = \rho_{r_0} - \int_0^t W_g \mathrm{d}y$$

and gaseous mass loss due to pyrolysis

$$\dot{m}_g = \int_0^L W_g \mathrm{d}y$$

where L is the wall thickness. Finally the recession rate is expressed in an empirical form

$$\dot{m} = \beta_1 \rho(T_s)^{\beta_2} \exp(-\beta_3/T_s)$$

where β's are constants and T_s is the surface temperature. The constants, β's, are function of material properties. For simple ablators, i.e., Teflon, whose decomposition kinetic are known, analytical expressions for β's can be obtained.[7] However, for the complex carbon phenolic ablator, the empirical constants from Ref. 6 will be used.

In formulating this model, we have made several assumptions. Firstly, the laser energy is assumed to be instantaneously absorbed at the surface. This implies that the absorption length in the solid is small compared with the thermal depth for the duration of interest. Secondly, when the phenolic resin decomposes at an elevated temperature which is below the sublimation temperature of carbon, the phenolic gas is assumed to be able to escape through the porous carbon char.

Now Eq. (1) can be solved with the appropriate initial and boundary conditions to provide complete temperature profiles in the solid and the surface recession rates. In the following calculations, the thermodynamic properties of carbon phenolic are taken from Ref. 6. The spectral emissivity of phenolic graphite which has been measured by Chang[8] varies from 0.87 in the visible spectrum to 0.62 in the infrared. However, as shown by Whitson,[9] the emissivity depends also on the type of graphite and its surface conditions. Here the emissivity of carbon phenolic is taken to be 0.81, and the initial temperature, T_0 has been assumed to be 300 K.

B. Coupling Coefficient

The calculation of impulse delivered per unit of incident energy, i.e., the "coupling coefficient," requires some knowledge of the phenomena above the solid surface. When the ambient pressure is either small or nonexisting we can assume that the gas at the surface has a Maxwellian velocity distribution. Then the mass flux per unit area leaving the surface can be readily expressed as a function of vapor pressure and temperature.[10] In the vacuum limit, $T_v = T_s$ and the vapor pressure can be obtained as $p_v = \dot{m}(2\pi R T_s)^{1/2}$. Once the vapor pressure is known, one can now calculate the instantaneous coupling coefficient $C = p_v/I$ and the integrated coupling coefficient

$$C_I = \int_0^t p_v \mathrm{d}t \Big/ \int_0^t I \mathrm{d}t$$

The definition of C_I is appropriate for comparison with experimental measurements of the net impulse delivered per unit of incident energy. For a sufficiently long laser pulse, the coupling coefficient will rise from zero at the beginning of the

Received Dec. 16, 1976; revision received March 3, 1977.
Index categories: Lasers; Combustion in Heterogeneous Media; Heat Conduction.

*Principal Scientist. Member AIAA.
†Principal Scientist.